FRACTURAL MODELLING OF EARLY-AGE CONCRETE BEAMS UNDER THREE-POIN LOADING

Xianyu Jin[1], Nanguo Jin[2], and Yanguo Zheng[3]

ABSTRACT

A finite element program, ABAQUS, is used to simulate the fractural behaviour of grade C30 concrete beams under a three-point loading configuration, at the ages of 1, 2, 7, and 28 days. Based on the Crack Band model, a bi-linear strain-softening curve was derived with the parameters determined by curve fitting for the three-point bending tests. The simulated LOAD-CMOD curve and the experimental results show a good agreement. Furthermore, the numerically simulated LOAD-CMOD curves also match the experimental LOAD-Displacement curves of the concrete beam at different ages. By applying the LEFM method, the critical stress intensity factor K_{Ic}^{s} and the critical crack tip opening displacement ($CTOD_c$) of concrete are determined and compared with those of the experimental values, and excellent agreement is found.

KEY WORDS

Early-age concrete, ABAQUS, stress-strain softening curve, critical stress intensity factor, fracture energy.

INTRODUCTION

Most of the cracks within concrete members were caused by thermal stress, self-shrinkage, drying shrinkage and external load. Therefore, the concrete structures were prone to fail before concrete hardening, which especially will affect the durability and service life. So it is very essential to give more attention to the cracking of early-concrete.

Many foregoing researches on early-concrete laid particular stress on the properties of material, but less on such mechanics behaviors as damage and fracture. In this paper, based on the two-parameters mode test recommended by RILEM, and by the general finite element code ABAQUS, a numerical analysis to the formation and propagation of cracks within early-concrete under external load was implemented.

TWO-PARAMETERS MODEL TEST

Materials and Mix Proportion

Cement: ASTM I Portland cement, with the density 3 150 kg/m^3, specific surface area 385

[1] Professor, Civil. Engrg. Department, Zhejiang Univ., Hangzhou, 310027, P.R. China, Phone +86 571/8795 2257, FAX 571/8795-2165, xianyu@zju.edu.cn

[2] Associate Professor, Civil. Engrg. Department, Zhejiang Univ., Hangzhou, 310027, P.R. China, Phone +86 571/8795-1397, FAX 571/8795-2165, jinng2005@yahoo.com.cn

[3] Senior Engineer,Nuclear power Qinshan Joint Venture Company Limited, Haiyan, 314300, P.R. China, Phone +86 573/6931-249, FAX 573/6402-560, zhengyg@npqjvc.cn.

m^2/kg, the average grain size 19.98μm; Fine aggregate: with the fineness modulus 2.3, the density of natural river sand 2 660 kg/m^3; Coarse aggregate: with the maximum grain size 10 mm, the density of crushed stone 2570 kg/m^3; Water: tap water. The mix proportion of this concrete is 0.55.

Experiment

At least four beams were tested in every group fracture with the specimen size 75 mm×150 mm ×750 mm, the depth of the notch a_0 50 mm, the width of the notch 3 mm. The span length S (the clear distance between two supports) is 600mm, and the depth of the three-point bending beam D is 150mm.More details can be seen in fig1. All the specimens expect one day age specimen were demoulded after one day, which then were cured under the temperature (23±2)℃ and the relative humidity 100%. The fracture test apparatus used here is MTS810, as shown in fig2. the maximum load 250kN can be gained and the crack mouth opening displacement (CMOD) was taken as the feedback to keep stabilization of the failure.

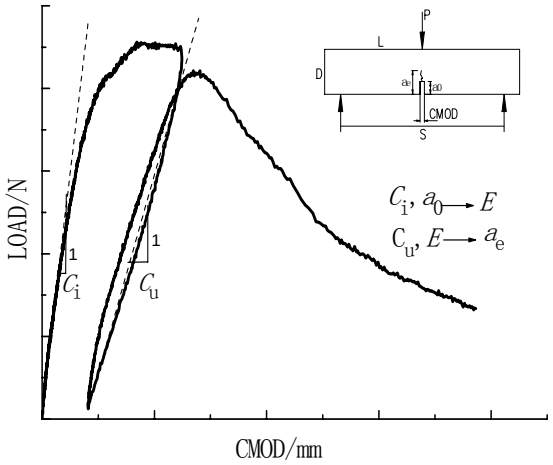

Figure 1: Specimen size and typical curve

Figure2: MTS810 apparatus

Two-parameter Model

In this model, the critical stress intensity, K_{IC}^{s}, the critical crack tip opening displacement $CTOD_c$ and the modulus of elasticity can be calculated as follows (Jenq and Shah,1985):

$$K_{IC}^{s} = \frac{3(P_{max} + 0.5WS/L)S}{2D^2B}\sqrt{\pi a_e}F(\alpha) \quad (1)$$

$$CTOD_c = \frac{6(P_{max} + 0.5WS/L)Sa_e}{D^2BE}V_1(\alpha)\{(1-\beta)^2 + (-1.149\alpha + 1.081)(\beta - \beta^2)\}^{1/2} \quad (2)$$

$$E = 6Sa_0V_1(\alpha)/(C_iD^2B) \quad (3)$$

where, S, a_0 , D, B is shown in fig1; C_i :the initial flexibility, $\alpha = (a_0 + H_0)/(D + H_0)$; H_0 : the thickness of the clamp; $V_1(\alpha)$: the shape function about α , $V_1(\alpha) = 0.76 - 2.28\alpha + 3.87\alpha^2 - 2.04\alpha^3 + 0.66/(1-\alpha)^2$; $P_{\max}$: the ultimate load; W : the self-weight of beam; a_e : the critical effective crack length: $a_e = EC_u D^2 B/(6SV_1(\alpha))$; C_u : the unloading flexibility; $F(\alpha)$: the shape function about α

$$F(\alpha) = [1.99 - \alpha(1-\alpha)(2.15 - 3.93\alpha + 2.7\alpha^2)]/[\sqrt{\pi}(1+2\alpha)(1-\alpha)^{3/2}]$$

where, $\alpha = a_e / D$; $\beta = a_0 / a_e$

The test results can be found in table 1.

Table 1: TPM results for concrete of C30

ages / d	$K_{IC}^s / (\mathrm{MPa} \bullet \mathrm{m}^{0.5})$	$CTOD_c$ / mm	$f_c^{'}$ / MPa
1 d	0.415	0.0109	10.46
2 d	0.707	0.0146	15.30
7 d	0.977	0.0143	25.66
28d	1.263	0.0159	35.97

More details about this test can be found in the literature(Xianyu Jin et al. 2005).

NUMERICAL ANALYSIS

The Finite Element Model

The crack band model proposed by Bazant (2002) was applied to take into account the element size effect of concrete. In the case of plane stress, when two cracks occurred on a gauss point of an element, along the cracking direction, the incremental form stress-strain relationship can be expressed as:

$$\begin{Bmatrix} \Delta\sigma_{nn} \\ \Delta\sigma_{tt} \\ \Delta\sigma_{nt} \end{Bmatrix} = \begin{bmatrix} k_{soft,1}E_0 & 0 & 0 \\ 0 & k_{soft,2}E_0 & 0 \\ 0 & 0 & \beta G_0 \end{bmatrix} \begin{Bmatrix} \Delta\varepsilon_{nn} \\ \Delta\varepsilon_{tt} \\ \Delta\varepsilon_{nt} \end{Bmatrix} \quad (4)$$

where , σ_{nn} and ε_{nn} are respectively the positive stress and strain of crack 1, while σ_{tt} and ε_{tt} are respectively the positive stress and strain of crack 2. σ_{nt} and ε_{nt} are respectively the shear stress and strain. The rest had such meanings as follows:

E_0 : the initial modulus of elasticity; G_0 : the initial modulus of shear; $k_{soft,1}$: the tension crack softening coefficient of crack 1; $k_{soft,2}$: the tension crack softening coefficient

of crack 2; β: shear transfer factor, and it reveals the interlocking action between the surfaces of the crack. Due to the experiment being type I fracture model, post-shear effect is neglected.

The conception of band width in this model was equal to the characteristic element length in ABAQUS, which is dependent of the element geometry shape: for beam and truss elements, it is the length between gauss points; for shell and plane elements, it is the square root of gauss points; for solid elements it is the cube root of gauss points. CPS4R(plane stress 4—node simplified integral element) in ABAQUS element family was adopted in this simulation, the sum of the elements and nodes are 3 702 and 3 905 respectively. A modified Riks iterative method was used here to find the descending branch. Fine gridding was adopted within the crack band and supports. The supports and the loading bar were simulated by analytical rigid bodies. The detailed gridding partitions are shown in fig3:

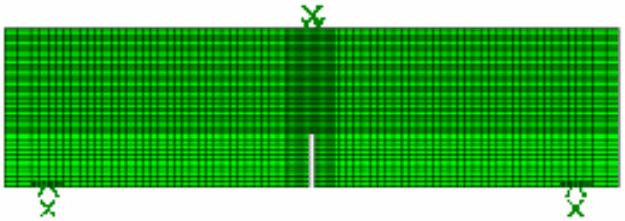

Figure 3: FEM of three-point bending beam

The Determination of Two-Linearly Tension Softening Curve

As we all know, there exists a fracture process zone in front of the crack tip, which will arouse a phenomenon termed as tension softening. This characteristic played an very important role on finding the ultimate load and the descending curve.

The primitive work was completed by Hillerborg, he suggested an exponential decay softening curve with the separate displacement *w* independent variable (see fig4). Thereafter, based on large amounts of experiments, Petersson gave an two-linearly softening curve, as is shown in fig5. Many succedent experiments and numerical analysis indicated that it is adequate for two-linearly curve to describe this softening phenomenon.

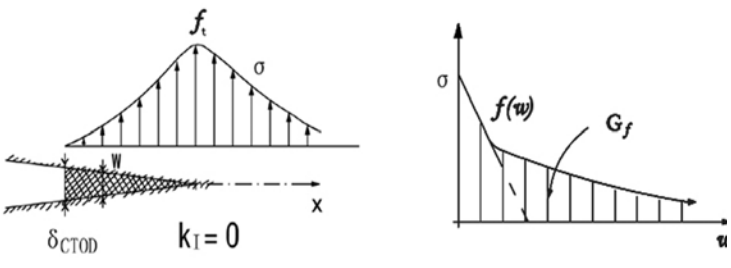

Figure 4: Stress distribution of FPZ and soften curve

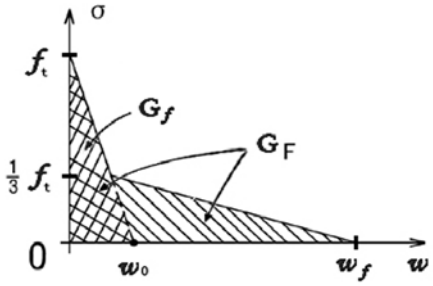

Figure 5: Two linearly tension soften stress —displacement curve

The stress value at the slope transition is usually taken as 0.15 f_t ～ $f_t/3$, and the area under the stress-separate displacement curve, denoted as $f(w)$, represents the required energy to develop every one unit area crack, denoted as G_F(N/m), while G_f represents the area under initial slope. Planas and Bazant et al.(1997) pointed out that it is the G_f that determines the ultimate load. The value of G_f in TPM is equal to the critical strain energy release rate, denoted as G_{IC}^s. Since the stress at slope transition was determined, with the values of G_F and G_f, the shape of the two-linearly tension softening curve could be gained. Assuming the stress at slope transition is ψf_t, two equations below can be easily got by area calculations:

$$W_0 = \frac{2G_f}{f_t} \tag{5}$$

$$W_f = \frac{2}{\psi f_t}\left[G_F - (1-\psi)G_f\right] \tag{6}$$

By trial and errors, Petersson's suggestion was adopted, that is, $\psi = 1/3$. Since G_F cannot be directly derived from the TPM test, it can only be got from conversion of K_{IC}^s directly gained from this test.

First, G_{IC}^S can be determined by the equation below:

$$G_{IC}^s = {K_{IC}^s}^2 / E \tag{7}$$

then, based on the conclusions proposed by Planas and Guinea ()1992, 1994), an approximate equation affirmed by Bazant and Becq－Giraudon et al.can be gained that

$$G_F \approx 2.5G_f = 2.5G_{IC}^s. \tag{8}$$

which had been taken as the optimal database among different labs including 238 series of tests in all.

As to G_F, based on the productions presented by Planas and Elices(1997), the follow expression can be taken as:

$$G_F = \alpha G_{IC}^s \tag{9}$$

where, $\alpha \geq 2$. In practice, assuming $G_F = 2.5\,G_f$. For the general ratio of tension strength to compression strength is 1/12 ～ 1/10, thus W_0 and W_f can be completely determined. In order to keep the fracture energy unique and avoid the gridding sensitivity, W_0 and W_f were adapted to the crack band width h (the characteristic element length in ABAQUS), and the equations（5）、（6）can be rewritten as:

$$\varepsilon_0 = \frac{2G_f}{f_t h} \tag{10}$$

$$\varepsilon_f = \frac{2}{\psi f_t h}\left[G_F - (1-\psi)G_f\right] \tag{11}$$

Results Analysis

Taking an 28d three-point bending concrete beam for example, its cracking process and nephograms of stress distribution are as follows:

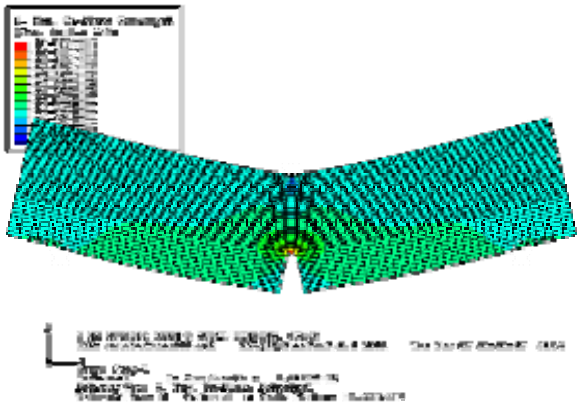

Figure 6: Initial cracking deformations and nephogram of the maximum principle stress

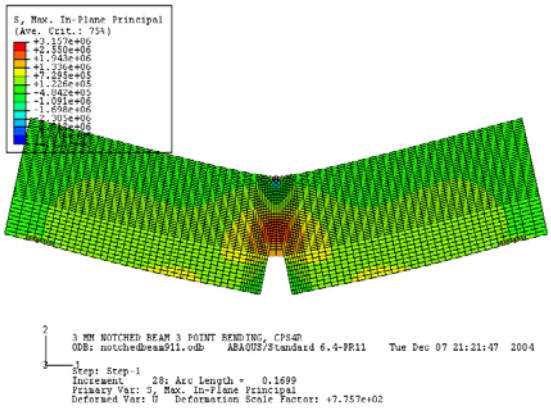

Figure 7: Cracking deformations of maximum load and nephogram of the maximum principle stress

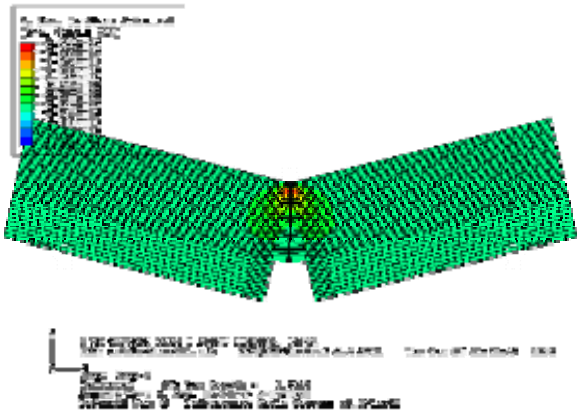

Figure 8: Ultimate cracking deformations and nephogram of the maximum principle stress

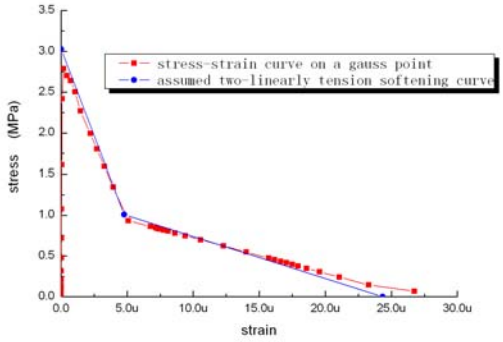

Figure 9: Stress—strain curve of the first element integral point above the notch

It can be seen from fig6,fig7 and fig8 that the opening displacement is gradually increasing and with the increasing load, the maximum tension stress is developing upwards into the ligament of beam along the notch. For the existence of the fracture process zone, the tension stress is not rapidly decreasing to zero, that is, a fraction of stress still remains. Taking out the first cracking element above the notch, draw a stress-strain curve of integral point as shown in fig9.

By the post output of ABAQUS, the 1、2、7、28d LOAD-CMOD comparison curves can be derived as fig10 shows:

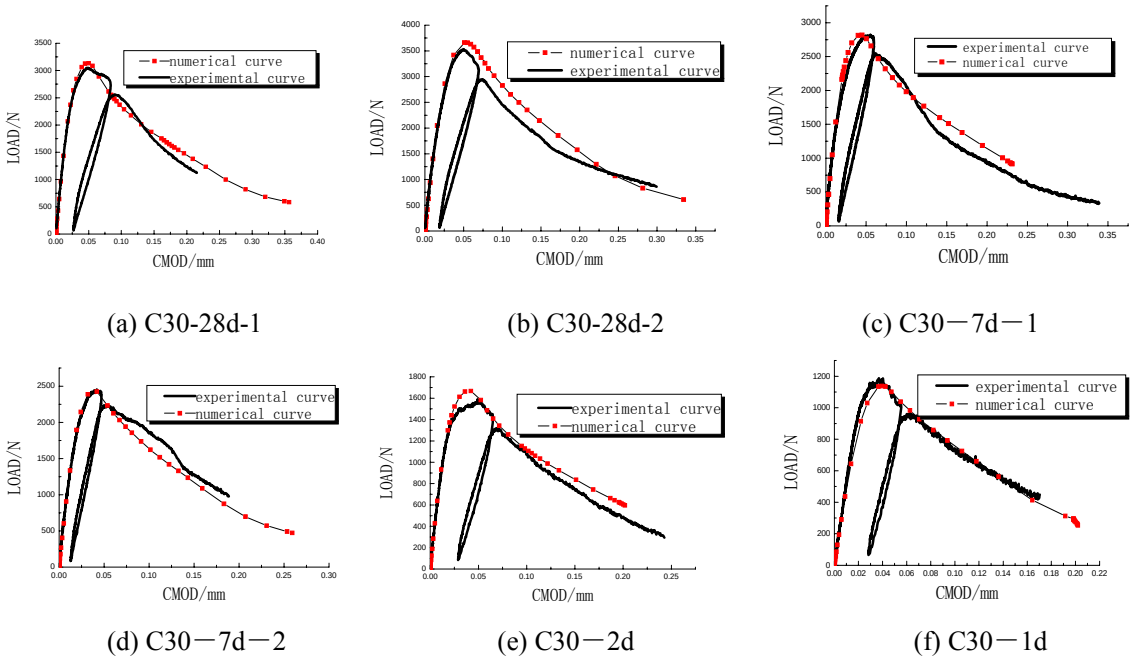

(a) C30-28d-1 (b) C30-28d-2 (c) C30－7d－1

(d) C30－7d－2 (e) C30－2d (f) C30－1d

Figure10: Comparisons between the simulated LOAD-CMOD curve and the experimental results

As is shown in fig10, in the ascending segment of the curves, the numerical results matched up to the test. However, as to the descending segment, it was not the case for such reasons as follows:

- Because of the uploading process occurring in the TPM test, energy loss cannot be avoided;
- The crack band theoretics assumes that G_F can only be dissipated by crack band, while all deformations out of this band are elastic, which cannot dissipate the fracture energy. However, it can be clearly seen from fig6,fig7 and fig8 that there did exist some plastic deformations near the supports, which by all means dissipated the fracture energy.

By making a contrast statistic to 1d~28d numerical and experimental results, it was found that the average error was merely about 3%, which indicated that the calculations of G_f that determines the ultimate load was relatively exact.

Make mutual comparisons of LOAD-CMOD curve and LOAD-Displacement curve among different ages, seeing fig11, fig12.

As is shown in the two figures above, in the stable crack propagation segment, that is, before the ultimate load reaches, the slope is increasing with the increment of the age. While, in the descending segment, that is, the unstable crack propagation segment, the load is rapidly descending with the age increasing. Especially the early-age concrete beam, for example, 1d beams, the load descending is relatively slow, which to some extent behave plasticity. These conclusions can also be found in Jin－Keun Kim(2004).

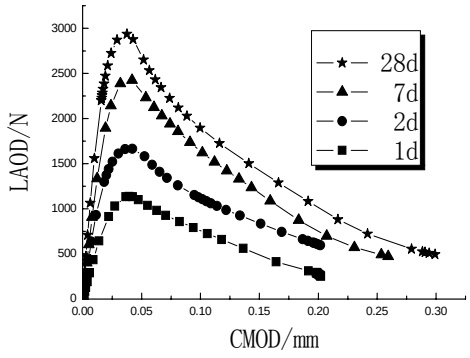

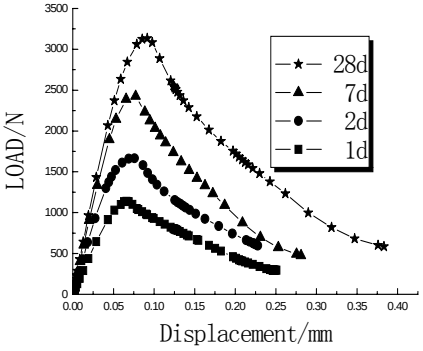

Figure11: Comparisons of LOAD-CMOD curves

Figure12: Comparisons of LOAD Displacement curves

The calculations of $K_{\mathrm{Ic}}^{\mathrm{s}}$ and $CTOD_c$ had been explained in the TPM test, and here another LEFM method will be applied to solve the equivalent elastic critical crack length a_{ce}. Consequently, $K_{\mathrm{Ic}}^{\mathrm{s}}$ and $CTOD_c$ can be gained by the crack opening displacement (COD) derived from simulations. The detailed processes are as follows:

- Based on LEFM manual, for the single side notched three-point bending beams (S＝4b), the following equations can be gained:

$$COD(a,x) = CMOD \times g_1(\frac{a}{b},\frac{x}{a}) \tag{12}$$

$$g_1(\frac{a}{b},\frac{x}{a}) = \left\{\left(1-\frac{x}{a}\right)^2 + \left(1.081-1.149\frac{a}{b}\right)\left[\frac{x}{a}-\left(\frac{x}{a}\right)^2\right]\right\}^{\frac{1}{2}} \tag{13}$$

where, x —the vertical distance away from the bottom of beams
b —depth of the beam
a —length of the crack
g —COD function of three-point bending beams（$S=4b$）.

- Taking a ＝65、70、75、80、85 (mm) respectively to make function curves as shown in fig13.
- Near the tip of the crack, the shape of the curves exhibit non-linearly, while it tends to be relatively linear far away from the tip.
- Along the notch, take turns to choose five nodes every 10mm from the first node at the bottom of beams, and thus the horizontal displacement of the first node is equal to half the *CMOD*. With the numerical results, values of *COD* for five nodes can be got when reaching the ultimate load, then bring the *CMOD* of the first node, along with random

COD of the rest four nodes, into the equation（13）, an non-linear equation can be derived about the crack length a, and it can be easily solved by the numerical iterative tool MATLAB. The solution a is the equivalent elastic critical crack length a_{ce} corresponding to the ultimate load. Then, bring another *COD* into the equation（13）, and another a_{ce} can be solved the same way. Take the average of this two a_{ce} and the final a_{ce} can be gained.

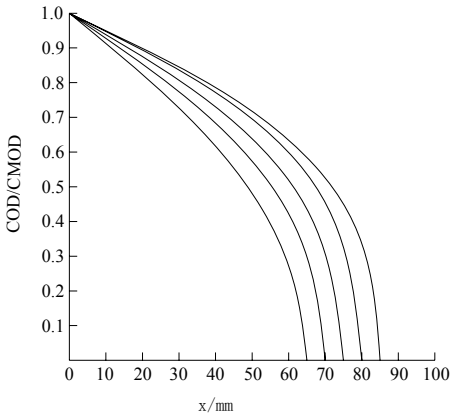

Figure 13: *COD* of three-point bending beam（s＝4b）

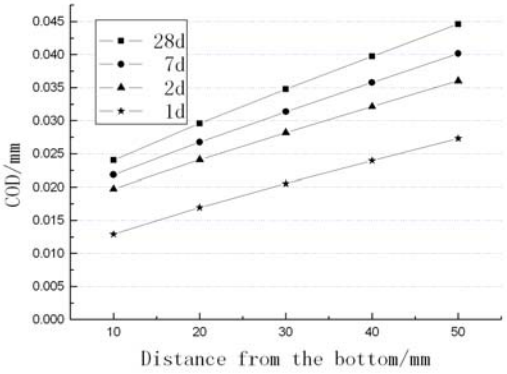

Figure 14: Comparisons of *COD* at peak load

- Based on LEFM, as to the three-point bending beam（S＝4b）, there is:

$$K_{IC} = \sigma_{max}\sqrt{\pi a_{ce}}\, g_1\left(\frac{a_{ce}}{b}\right), \quad \sigma_{max} = \frac{3P_{max}S}{2b^2t} \tag{14}$$

$$g_2\left(\frac{a}{b}\right) = \frac{1.99-(a/b)(1-a/b)\left[2.15-3.93a/b+2.70(a/b)^2\right]}{\sqrt{\pi}(1+2a/b)(1-a/b)^{3/2}} \tag{15}$$

where, S —net span of beams; t — thickness of beams; b —depth of beams

Taking the solved a_{ce} and the numerical results P_{max} into the equation（15）, K_{IC}^{s} can be calculated. Taking the a_{ce}, $x = 50$ mm and *CMOD* into the equation （13）, $CTOD_c$ can be solved.

Taking a 1d concrete beam of grade C30 for example, repeat the calculating process as follows: numerical P_{max}＝1 138N（practical P_{max}＝1 186.699N）, $x = 0$, $CMOD$＝3.661 28×10^{-2}mm; $x = 10$ mm, COD＝3.240 92×10^{-2}mm; $x = 20$ mm, COD＝2.814 44×10^{-2}mm. Bring these into the equation（13）and solve this non-linear equation, it is gained that $x = 10$, a_{ce}＝61.185 8; $x = 20$, a_{ce}＝61.898 3. Thus the average $\overline{a_{ce}}$＝61.542mm. The practical $\overline{a_{ce}}$ derived from the TPM test is 62.512 mm, and the relative error is 1.6%. Bring $\overline{a_{ce}}$＝61.542 mm, P_{max}＝1138N into the equation（15）, K_{IC}^{s}＝0.325 6（MPa*m$^{0.5}$）can be solved. The practical K_{IC}^{s} is 0.364 5（MPa*m$^{0.5}$）, and the relative error is 10.67%.

Bring $\overline{a_{ce}}$ =61.542mm, $CMOD$=3.661 28×10^{-2}mm, $x = 50$ mm into the equation（13）, $CTOD_c$ =0.013 102 mm can be solved. The practical $CTOD_c$ is 0.011 689 74mm, and the relative error is 12.1%. Draw a *COD* curves when reaching the ultimate load as shown in fig14.

CONCLUSIONS

- The numerical results agreed well with the experimental values, and the differences among different ages accorded with the experiment and correlated productions of literatures.
- Using the LEFM method to validate the two parameters of TPM test, it was found that the numerical predictions closely match those of the experimental values, which confirms the validity of the FEA programs.
- By successfully carrying out the finite element analysis of beams on a three-point bending configuration as reported in this paper, a powerful numerical analytical tool has been identified for the investigation of fractural behaviour of damage and fracture in early-age concrete members.

ACKNOWLEDGEMENTS

The financial support of the National Natural Science Foundation of China (NSFC50578142) is greatly acknowledged.

REFRENCES

Jenq Y S, Shah S P(1985). ”Two parameter fracture model for Concrete”, *J.Journal of Engineering Mechanics,* 111(10) 1227-1241.

Jin Nanguo, Jin Xian-yu, Zheng Yanguo,et al(2005). ”Experimental study on fracture properties and microstructure of concrete at early age”, *J.Journal of Zhejiang University: engineering science*, 39(9) 1374-1377.

Bazant Z P(2002). ”Concrete fracture models:testing and practice”, *J, Engineering Fracture Mechanics*, 69(2) 165-205.

Bazant Z P, Planas J(1997). Fracture and size effect in concrete and other quasibrittle materials, Boca Baton, CRC Press.

Planas J,Elices M, Guinea G V(1992). ”Measurement of the fracture energy using three-point bend test: Part2-Influence of bulk energy dissipation”, *J.Mater Struct*,25(4) 12-305.

Guinea G V,Planas J, Elices M(1994). ”A general bilinear fit for the softening curve of concrete”, *J.Mater Struct*, 27(1) 99-105.

Bazant Z P,Becq-Giraudon E(). ”Statistical prediction of fracture parameters of concrete and comparison of testing methods”, *J.Cement Concrete Res*,in press.

Guinea G V, Elices M ,Planas J(1997). ”On the initial shape of the softening function of cohesive materials”, *J.Int J Fract*,87(1) 49-139.

Kim Jin-keun, Lee Yun(2004). ”Yi Seong-tae. Fracture characteristics of concrete at early ages”, *J.Cement and Concrete research* ,34(3) 507-519.